New Iron Hydrides under High Pressure

Charles M. Pépin,* Agnès Dewaele, Grégory Geneste, and Paul Loubeyre†
CEA, DAM, DIF, F-91297 Arpajon, France

Mohamed Mezouar
ESRF, 6 Rue Jules Horowitz BP220, F-38043 Grenoble Cedex, France

(Received 25 July 2014; revised manuscript received 13 November 2014; published 30 December 2014)

The Fe-H system has been investigated by combined x-ray diffraction studies and total energy calculations at pressures up to 136 GPa. The experiments involve laser annealing of hydrogen-embedded iron in a diamond anvil cell. Two new FeH_x compounds, with $x \sim 2$ and $x = 3$, are discovered at 67 and 86 GPa, respectively. Their crystal structures are identified (unit cell and Fe positional parameters from x-ray diffraction, H positional parameters from *ab initio* calculations) as tetragonal with space group $I4/mmm$ for $FeH_{\sim 2}$ and as simple cubic with space group $Pm\bar{3}m$ for FeH_3. Large metastability regimes are observed that allowed to measure the $P(V)$ equation of state at room temperature of FeH, $FeH_{\sim 2}$, and FeH_3.

DOI: 10.1103/PhysRevLett.113.265504 PACS numbers: 81.40.Vw, 88.85.mh

Under pressure, most transition metals form hydrides, usually with a H:metal ratio close to 1 [1]. But this view of chemical combination should be considerably expanded by going in the 100 GPa pressure range. Indeed, a rough rule emerges from numerous first-principles calculations on the reaction of H_2 with various normal and transition metals, namely, that the hydrogen content of their hydrides should significantly increase with pressure. Therefore, predictions of polyhydrides with unusual stoichiometries abound such as LiH_2, LiH_6 [2], NaH_9 [3], CaH_6 [4], FeH_3, and FeH_4 [5]. Up to now, this remarkable high pressure behavior of hydrides has been awaiting clear experimental confirmation. In this Letter we show that under pressure the hydrogen content in Fe dramatically increases through discontinuous steps, leading to the formation of two new FeH_x compounds: $FeH_{\sim 2}$, composed by alternate layers of atomic H and of Fe, and FeH_3.

Pure Fe and H_2 solids have been extensively studied under pressure over the past 30 years, disclosing very intriguing properties [6,7]. The study of FeH_x compounds could be as interesting. By significantly varying the Fe:H ratio in the iron hydrides, one can expect the properties of FeH_x to be tuned from ironlike to hydrogenlike. On the one hand, the phase diagram of FeH is related to the one of pure iron, with a face-centered cubic (fcc) structure under P-T conditions similar to the stability field of fcc Fe [8,9] (see Fig. 1). Also, FeH is ferromagnetic at low pressures and undergoes a magnetic collapse around 22 GPa [10], at a slightly higher pressure than the one in Fe. On the other hand, hydrogen rich compounds should have analogous properties to those of metallic hydrogen and so hold promise as high temperature superconductors [11], with predictions of superconductivity critical temperature as high as 220 K in CaH_6 [4]. As such, hydrogenlike properties could be expected for $FeH_{x>1}$ compounds. Apart from these fundamental issues, the observed stability of novel iron hydrides under high pressure should have a significant impact on planetary interior modeling since Fe and H are two of their main constituents [12,13]. In particular, hydrogen is considered as a possible light element in Earth's core, which is mainly composed of iron [14].

Previous diamond anvil cell (DAC)-based pressure studies of hydrides were performed at 300 K. Only three polyhydrides of transition metals have been observed by doing so: rhodium dihydride [15], tungsten hydride [16], and iridium trihydride [17]. The present experiments have been performed by laser heating hydrogen-embedded Fe

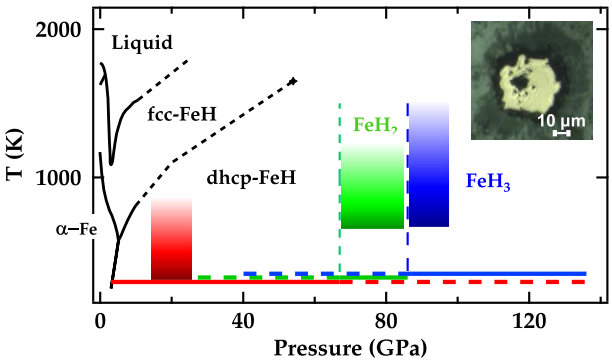

FIG. 1 (color online). Phase diagram of the Fe-H system. The black boundary lines for FeH have been taken from Refs. [8] and [9]. Colored rectangles depict the P-T regions where laser heating has been performed and the stability domains of dhcp-FeH, FeH_2, and FeH_3 are indicated. Horizontal solid and dashed lines indicate the pressure range over which these phases are stable and metastable, respectively, at 298 K. Inset: photograph of a typical sample configuration. The sample is embedded in hydrogen and sits on c-BN grains, the small black dots which can also be seen around it.

samples in the 100 GPa pressure range at temperatures between 300 and 1500 K. A very slow transformation kinetics exists in hydrogen-metal systems and, consequently, heating is mandatory to explore the stability field of polyhydrides under pressure.

Experiments were performed on 2 μm thick Fe polycrystalline samples loaded in diamond anvil cells with hydrogen as a pressure medium. Rhenium gaskets have been used, protected with a 800 Å gold coating to prevent the loss of hydrogen by diffusion. Pressure was measured using the equation of state of a small piece of gold [18] loaded close to the sample. Powder diffraction patterns were analyzed using the FULLPROF software. The uncertainty in volume is ± 0.05 cm^3/mol and in pressure $\pm 2\%$. YAG-laser heating of the sample, with an on-line setup on the ID27 x-ray diffraction (XRD) beam line (angular dispersive mode) of the European Synchrotron Radiation Facility, has been performed at several pressures: 12, 17, 27, 67, 70, 84, 86, and 90 GPa, keeping the temperature below 1500 K. The P-T phase diagram's space so explored is represented in Fig. 1. The Fe sample was thermally insulated from the diamond culets either by thin layers of KCl, LiF ($\sim$2 μm, pressed onto each diamond before loading) or grains of c-BN. Experimental runs performed with these different sample assemblies gave consistent results, which proves that no parasitic chemical reaction with the insulating media or the diamond culet occurred. Because of the difficulty of laser heating in a hydrogen environment, because of its high reactivity [19,20] and increased diffusivity often resulting in the failure of the diamond anvils, XRD data were taken before and $\sim$1 min after heating, but not during heating.

The Fe-H system has already been substantially studied up to 80 GPa and FeH is the only stoichiometry observed so far [8,9,21]. In the first part of this work, we revisit and extend the cold compression curve of double hcp (dhcp)-FeH up to 136 GPa. Four runs were performed. In three of them, a laser annealing of the sample during $\sim$3 min was made at 12, 17, and at 27 GPa, respectively, keeping the temperature below the transition to fcc-FeH ($T \leq 1000$ K) (see Fig. 1). No phase nor volume change was observed after the heating cycle. Such laser heating enables us to significantly improve the sample crystalline quality, evidenced by sharper XRD lines, and, hence, to reduce the experimental uncertainty in the volume determination. A diffraction pattern is plotted in Fig. 2, typical of those in the 100 GPa pressure range. Our $V(P)$ data points are plotted in Fig. 3 together with literature data [22,23], with a good agreement. The present data are less scattered thanks to the improved volume accuracy. The $V(P)$ data points are fitted with a Vinet-type equation of state [24], yielding the zero pressure volume, the bulk modulus, and its pressure derivative. These values are reported in Table I. In a previous study, an anomalous compressibility behavior above 50 GPa was interpreted as a slight increase of the

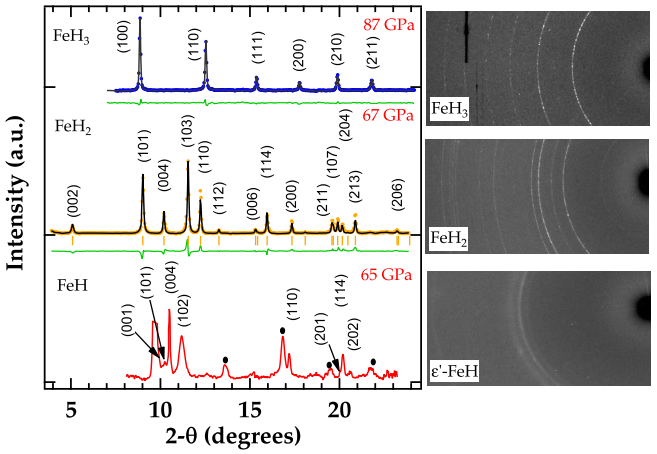

FIG. 2 (color online). X-ray diffraction patterns of FeH, FeH_2, and FeH_3 (right: image plates, left: integrated patterns). Bottom: dhcp-FeH at 64 GPa. Black dots mark the diffraction peaks from insulating material KCl. The significant broadening of the (102) peak relative to the others is attributed to random stacking faults [23]. Middle: FeH_2 at 67 GPa, described as a tetragonal $I4/mmm$ ($a = 2.479$ Å, $c = 8.415$ Å, $Z = 4$) unit cell, Fe in positions 4e (0,0,0.853). The Rietveld refinement is shown with a Bragg R factor $R_B = 12.1\%$. Top: Simple cubic $Pm\bar{3}m$ ($a = 2.437$ Å, $Z = 1$) phase of FeH_3 at 87 GPa. The Rietveld refinement with Fe in positions 1a (0,0,0) is shown with a Bragg R factor $R_B = 8.4\%$.

H concentration [23]. Such behavior is not observed here. Also, theoretical calculations have predicted two phase transitions below 100 GPa, first toward an hcp lattice and then to a fcc lattice [25] but none are observed here even by going up to 136 GPa. We thus conclude that under cold compression, there is no change of the H content nor of the structure of dhcp-FeH, even by going up to 136 GPa.

Laser heating between 67 and 86 GPa leads to the disappearance of the dhcp-FeH XRD peaks. The Rietveld refinement of the integrated new diffraction pattern after heating at 67 GPa shown in Fig. 2 gives a tetragonal unit cell with the symmetry $I4/mmm$ and four iron atoms in Wycoff positions 4e (0, 0, 0.853). Because of the low atomic scattering power of H, it is impossible to determine the exact stoichiometry and the H atoms positions using the XRD data. At 67 GPa, the volume per Fe atom is 12.93 Å^3, i.e., $\sim$4 Å^3 larger than the one in pure Fe and $\sim$2 Å^3 larger than the one in dhcp-FeH at the same pressure. This $\Delta V \simeq 2$ Å^3 is very close to the value determined from the volume expansion in the formation of 3d metal monohydrides [1]. Assuming a constant volume expansion upon the stoichiometry increase of 1 in FeH_x, we propose that this new phase is $FeH_{\sim 2}$. Also, as seen in Fig. 3, the volume per formula unit of $FeH_{\sim 2}$ is smaller than the one of ideal mixing of Fe and H_2 solids at the same pressure, as expected for a compound formation at high pressure. Annealing conditions ($T \simeq 1000$ K) were necessary to overcome kinetic barrier in the formation of $FeH_{\sim 2}$, which explains why it has not been observed before [23]. At

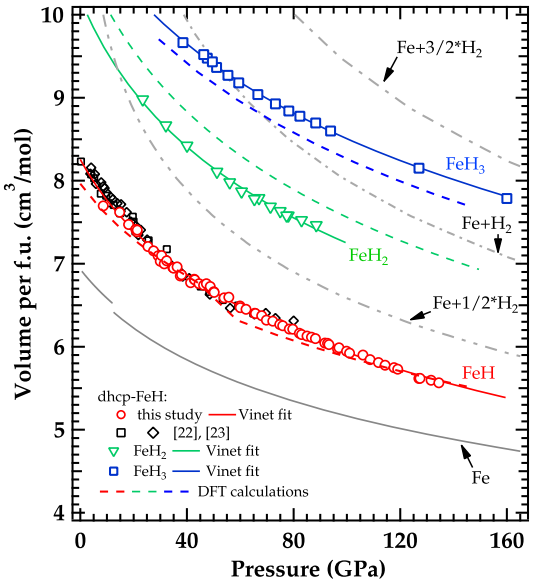

FIG. 3 (color online). Molar volume per formula unit as a function of pressure for iron hydrides. Experimental data for dhcp-FeH, $FeH_{\sim 2}$, and FeH_3 are represented together with literature data for FeH [22,23]. Error bars do not exceed the size of the data points. The Vinet fits [24] of the data are full lines and correspond to the parameters given in Table I. Dashed lines are results from the *ab initio* calculations with the most stable magnetic order (see text). Dash-dotted lines depict the molar volumes of ideal mixtures of iron and hydrogen with H:Fe ratio of 1, 2, and 3 using the equations of state of Refs. [26,27].

ambient temperature, FeH_2 is preserved upon pressure decrease down to 23 GPa and so its equation of state could be measured by going down in pressure (see Fig. 3). These data points are fitted by a Vinet-type equation of state, with the ambient pressure volume, bulk modulus, and its pressure derivative given in Table I.

A second compound replaces FeH_2 under laser heating at ~1400 K above 87 GPa, as shown in Fig. 2. The structural determination gives a simple cubic unit cell with the symmetry $Pm\bar{3}m$ [with one Fe atom in Wycoff positions $1a$ (0, 0, 0)], and a volume of 14.48 Å^3 per Fe atom at 87 GPa, that is ~2 Å^3 larger than the one in $FeH_{\sim 2}$ at the same pressure. This volume expansion being very near to the one in going from FeH to $FeH_{\sim 2}$, this new phase is thus likely to have an FeH_3 stoichiometry. Moreover, the measured volume and the positional parameters of Fe atoms are almost identical to those of the FeH_3 compound recently predicted by Bazhanova *et al.* [5], in which the H atoms are in positions $3c$ $(0, \frac{1}{2}, \frac{1}{2})$. The same structure has been observed for IrH_3, for the Ir/H system at high pressure [17]. At ambient temperature, FeH_3 can be preserved down to at least 39 GPa and was compressed up to 160 GPa. Its compression curve was measured over this pressure range, as shown in Fig. 3 and the parameters of the Vinet-type fit [24] of these data are reported in Table I.

First-principles density functional calculations using the ABINIT code [29] and the projector-augmented wave [30] method have been used to determine the structural positional parameters of the hydrogen atoms in FeH_2, and to calculate the properties of dhcp-FeH, FeH_2, and FeH_3. In particular, the calculated equation of state is used below to validate the $x \sim 2$ and $x = 3$ concentrations attributed to the two FeH_x compounds discovered. We employed the generalized gradient approximation in the Perdew-Burke-Ernzerhof form (GGA-PBE) [31]. The lattice parameters and atomic positions in the different phases have been optimized, providing in each case the enthalpy at $T = 0$ K as a function of hydrostatic pressure. The calculations do not take into account the zero-point energy. For each phase, both non-spin-polarized and spin-polarized calculations in a ferromagnetic (FM) configuration have been performed. In particular, for FeH_2, we started from the experimental determination of the space group and atomic positions of the Fe atoms (4 Fe/conventionnal cell) and we tested all the possibilities compatible with the Wyckoff positions of

TABLE I. Parameters (V_0: volume, K_0: bulk modulus, K_0': its pressure derivative, all at ambient conditions) of the equation of state obtained by the Vinet fit [24] of the experimental and *ab initio* data for Fe, FeH, FeH_2, and FeH_3. Numbers between parentheses represent fitting or published errors bars. FM: ferromagnetic; NM: nonmagnetic.

Phase	V_0 (cm^3/mol)	K_0 (GPa)	K_0'	Reference
Fe	6.754(0.015)	163.4(7.9)	5.38(0.16)	[26]
FeH	8.371(0.03)	131.1(3.0)	4.83	Experimental
	7.960(0.004)	185.2(0.5)	4.91(0.02)	*ab initio*, FM
	7.58(0.05)	227.2(0.02)	4.8(0.1)	*ab initio*, NM
	8.325(0.03)	150.0(5.0)	4	[23]
	8.371(0.07)	121.0(19.0)	5.31(0.9)	[22]
	8.244	155	3.7	[28], FM
	7.642	248	4.3	[28], NM
FeH_2	10.221(0.108)	127.2(8.1)	5	Experimental
	10.782(0.07)	127.0(0.1)	4.69(0.01)	*ab initio*, FM
FeH_3	11.171(0.04)	190.1(0.05)	5	Experimental
	10.858(0.003)	205.5(0.7)	4.38(0.01)	*ab initio*, NM

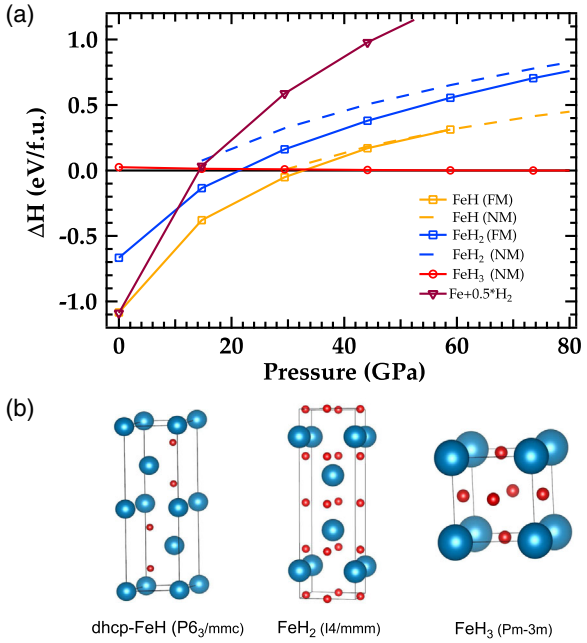

FIG. 4 (color online). (a) Calculated enthalpies as a function of pressure for the Fe-H structures proposed to match the experimental data. The magnetic phase of FeH_3 has been taken as reference so that $\Delta H = H(FeH_{3-n}) + (n/2)H(H_2)\text{-}H(FeH_3{}^{FM})$. (b) Representation of the structures of FeH, FeH_2, and FeH_3. Large blue and small red spheres represent the iron and hydrogen atoms, respectively.

space group $I4/mmm$. The structure, obtained at 67 GPa by placing 8 H atoms in the $4c$ $(0, \frac{1}{2}, 0)$ and $4d$ $(0, \frac{1}{2}, \frac{1}{4})$ positions, is the most stable, with relaxed cell parameters very close to the one measured at the same pressure. This structure is drawn in Fig. 4(b). It contains alternating layers of only Fe atoms and of only H atoms along the z direction. In FeH, a ferromagnetic to nonmagnetic transition is calculated to take place around 45 GPa, in good agreement with the predictions of Refs. [28,32]. In FeH_2, the ferromagnetic order is the most stable over the pressure range investigated here, with an even stronger effect on the enthalpy and on the equation of state than for FeH. In FeH_3, on the contrary, a ferromagnetic order appeared to have very little influence [Fig. 4(a)]. All structures were found to be metallic in the studied pressure range.

The calculated compression curves computed for FeH, FeH_2, and FeH_3 at $T = 0$ K are compared to experimental data in Fig. 3 and Table I. For FeH (with the FM to NM transition fixed around 45 GPa) and FeH_3, the calculated equilibrium volume and bulk moduli are, respectively, slightly lower and higher than the experimental ones, but the compression curves remain close in the scanned pressure range. These trends are similar to what is obtained for pure transition metals when the same GGA-PBE functional is used [33]. The inclusion of thermal expansion and zero point energy in the calculation could reduce the small difference. In contrast, the calculated compression curve for FeH_2 at $T = 0$ K is above the experimental one. This could be a hint that the H:Fe ratio is slightly below 2 in the phase observed experimentally, which is possible if the proposed structure contains hydrogen vacancies.

The calculated enthalpies of the various phases of Fe-H systems observed here are compared in Fig. 4(a). They are plotted relative to the one of $FeH_3{}^{FM}$. The sequence of stable phases under pressure according to the present calculation is $Fe + H_2$, dhcp-FeH with FM order, and cubic FeH_3. FeH_2 is never energetically favored over dhcp-FeH even when a ferromagnetic order is taken into account, although it significantly stabilizes this phase. Inclusion of the zero point energy of H_2 molecules would tend to stabilize phases with high hydrogen stoichiometries over those with low hydrogen stoichiometries, and thus would favor FeH_2 compared to FeH. The enthalpy of FeH_2 could also be lowered if this phase contains H vacancies, as discussed above.

FeH and FeH_2 both exhibit a smaller bulk modulus than the one of pure iron, whereas FeH_3 has a greater bulk modulus (see Table I). It is interesting to note that FeH_3 and IrH_3 [17] have the same structure and an equal bulk modulus of 190 GPa, although the bulk modulus of their parent metals are very different, 163 and 383 GPa for Fe and Ir, respectively. This could suggest that the properties of these two hydrides are strongly influenced by the properties of the H sublattice. This has already been discussed for metal AlH_3 in which the electronic properties could be described as the ones of the hydrogen sublattice weakly perturbed by Al atoms [34]. To what extent hydrides with a high H:metal ratio are analogous to metal hydrogen is of great fundamental interest. At 110 GPa, the H-H nearest distance is 1.70 Å in FeH_3, significantly larger than the 1.54 Å value in AlH_3 [35] but shorter than the 1.84 Å value in IrH_3 [17]. In these hydrides, the H-H distance diminishes slowly with pressure, going to 1.66 Å in FeH_3 at 160 GPa. To reach the 1.0 Å H-H distance expected for metal hydrogen at 450 GPa [36] would require pressures of ~850 GPa. On the other hand, the layer of atomic H in FeH_2 or the H sublattice in FeH_3 could have interesting properties analogous to those of expanded metal hydrogen. In addition, FeH_3, nonferromagnetic above 40 GPa, is calculated to be metallic: it would be very interesting to investigate if it is a superconductor as it has been proposed for hydrogen dominant alloys [11].

To sum up, we have synthesized two novel Fe hydrides, $FeH_{x\sim2}$ at 67 GPa and FeH_3 at 86 GPa, thus providing the first experimental confirmation of the theoretically predicted trend of an increase of hydrogen content in hydrides with increasing pressure. We observe a large metastability of the Fe-H compounds and laser heating was necessary to achieve the synthesis of $FeH_{x\sim2}$ and FeH_3. The search of FeH_4 and even higher stoichiometry iron hydrides now looks promising and a strong motivation to extend the present work to Earth's core conditions. The investigation

of the electronic properties of these novel iron compounds should now be very interesting with operative effects of magnetism, dimensionality, proton zero point energy, and correlations.

The authors acknowledge the European Synchrotron Radiation Facility for provision of synchrotron radiation on beam line ID27 (proposal HC-839). We wish to thank S. Anzellini, V. Svitlyk and P. Parisiadis for their help with the XRD experiments, and Z. Bazhanova for an exhange on the FeH_2 calculation.

*charles.pepin@cea.fr
†paul.loubeyre@cea.fr

[1] Y. Fukai, *The Metal-Hydrogen System: Basic Bulk Properties*, 2nd ed. (Springer, Berlin, 2005), Chap. 4.
[2] E. Zurek, R. Hoffmann, N. Ashcroft, A. Oganov, and A. Lyakhov, Proc. Natl. Acad. Sci. U.S.A. **106**, 17640 (2009).
[3] P. Baettig and E. Zurek, Phys. Rev. Lett. **106**, 237002 (2011).
[4] H. Wang, J. S. Tse, K. Tanaka, T. Iitaka, and Y. Ma, Proc. Natl. Acad. Sci. U.S.A. **109**, 6463 (2012).
[5] Z. Bazhanova, A. Oganov, and O. Gianola, Phys. Usp. **55**, 489 (2012).
[6] S. S. Saxena and P. B. Littlewood, Nature (London) **412**, 290 (2001).
[7] J. M. MacMahon, M. A. Morales, C. Pierleoni, and D. M. Ceperley, Rev. Mod. Phys. **84**, 1607 (2012).
[8] K. Sakamaki, E. Takahashi, Y. Nakajima, Y. Nishihara, K. Funakoshi, K. Suzuki, and Y. Fukai, Phys. Earth Planet. Inter. **174**, 192 (2009).
[9] O. Narygina, L. Dubrovinsky, C. McCammon, A. Kurnosov, I. Kantor, V. Prakapenka, and N. Dubrovinskaia, Earth Planet. Sci. Lett. **307**, 409 (2011).
[10] W. Mao, W. Sturhahn, D. Heinz, H. Mao, J. Shu, and R. Hemley, Geophys. Res. Lett. **31**, L15618 (2004).
[11] N. W. Ashcroft, Phys. Rev. Lett. **92**, 187002 (2004).
[12] D. Stevenson, Nature (London) **268**, 130 (1977).
[13] S. M. Wahl, H. F. Wilson, and B. Militzer, Astrophys. J. **773**, 95 (2013).
[14] J.-P. Poirier, Phys. Earth Planet. Inter. **85**, 319 (1994).
[15] B. Li, Y. Ding, D. Y. Kim, R. Ahuja, G. Zou, and H. K. Mao, Proc. Natl. Acad. Sci. U.S.A. **108**, 18618 (2011).
[16] T. Scheler, F. Peng, C. L. Guillaume, R. T. Howie, Y. Ma, and E. Gregoryanz, Phys. Rev. B **87**, 184117 (2013).
[17] T. Scheler, M. Marques, Z. Konopkova, C. L. Guillaume, R. T. Howie, and E. Gregoryanz, Phys. Rev. Lett. **111**, 215503 (2013).
[18] A. Dewaele, P. Loubeyre, and M. Mezouar, Phys. Rev. B **70**, 094112 (2004).
[19] T. Matsuoka, H. Fujihisa, N. Hirao, Y. Ohishi, T. Mitsui, R. Masuda, M. Seto, Y. Yoda, K. Shimizu, A. Machida *et al.*, Phys. Rev. Lett. **107**, 025501 (2011).
[20] N. Subramanian, A. F. Goncharov, V. V. Struzhkin, M. Sommayazulu, and R. J. Hemley, Proc. Natl. Acad. Sci. U.S.A. **108**, 6014 (2011).
[21] V. Antonov, E. Cornell, V. Fedotov, A. Kolesnikov, E. Ponyatovsky, V. Shiryaev, and H. Wipf, J. Alloys Compd. **264**, 214 (1998).
[22] J. V. Badding, R. Hemley, and H. Mao, Science **253**, 421 (1991).
[23] N. Hirao, T. Kondo, E. Ohtani, and K. Takemura, Geophys. Res. Lett. **31**, L06616 (2004).
[24] P. Vinet, J. Ferrante, J. Smith, and J. Rose, J. Phys. C **19**, L467 (1986).
[25] E. Isaev, S. Skorodumova, R. Ahija, Y. Velikov, and B. Johanson, Proc. Natl. Acad. Sci. U.S.A. **104**, 9168 (2007).
[26] A. Dewaele, P. Loubeyre, F. Occelli, M. Mezouar, P. I. Dorogokupets, and M. Torrent, Phys. Rev. Lett. **97**, 215504 (2006).
[27] P. Loubeyre, R. LeToullec, D. Hausermann, M. Hanfland, R. Hemley, H. Mao, and L. Finger, Nature (London) **383**, 702 (1996).
[28] C. Elssser, J. Zhu, S. Louie, B. Meyer, M. Fähnle, and C. Chan, J. Phys. Condens. Matter **10**, 5113 (1998).
[29] X. Gonze, G. M. Rignanese, M. Verstraete, J. M. Beuken, Y. Pouillon, R.Caracas, F. Jollet, M. Torrent, G. Zerah, M. Mikami *et al.*, Z. Kristallogr. **220**, 558 (2005).
[30] M. Torrent, F. Jollet, F. Bottin, G. Zerah, and X. Gonze, Comput. Mater. Sci. **42**, 337 (2008).
[31] J. P. Perdew, K. Burke, and M. Ernzerhof, Phys. Rev. Lett. **77**, 3865 (1996).
[32] T. Tsumuraya, Y. Matsuura, T. Shishidou, and T. Oguchi, J. Phys. Soc. Jpn. **81**, 064707 (2012).
[33] A. Dewaele, M. Torrent, P. Loubeyre, and M. Mezouar, Phys. Rev. B **78**, 104102 (2008).
[34] I. G. Gurtubay, B. Rousseau, and A. Bergara, Phys. Rev. B **82**, 085113 (2010).
[35] I. Goncharenko, M. I. Eremets, M. Hanfland, J. S. Tse, M. Amboage, Y. Yao, and I. A. Trojan, Phys. Rev. Lett. **100**, 045504 (2008).
[36] J. M. McMahon and D. M. Ceperley, Phys. Rev. Lett. **106**, 165302 (2011).